Size-dependent surface plasmon resonance in silver silica nanocomposites



2008 Nanotechnology 19 075710

(http://iopscience.iop.org/0957-4484/19/7/075710)

Nanotechnology **19** (2008) 075710 (7pp) doi:10.1088/0957-4484/19/7/075710

# Size-dependent surface plasmon resonance in silver silica nanocomposites

**Senoy Thomas[1], Saritha K Nair[1], E Muhammad Abdul Jamal[1], S H Al-Harthi[2], Manoj Raama Varma[3] and M R Anantharaman[1,4]**

[1] Department of Physics, Cochin University of Science and Technology, Cochin 682022, India
[2] Department of Physics, College of Science, Sultan Qaboos University, Sultanate of Oman
[3] National Institute for Interdisciplinary Sciences and Technology, Thiruvananthapuram, India

E-mail: senoythomas@yahoo.co.in and mra@cusat.ac.in

Received 7 September 2007, in final form 26 November 2007
Published 31 January 2008
Online at stacks.iop.org/Nano/19/075710

**Abstract**

Silver silica nanocomposites were obtained by the sol–gel technique using tetraethyl orthosilicate (TEOS) and silver nitrate ($AgNO_3$) as precursors. The silver nitrate concentration was varied for obtaining composites with different nanoparticle sizes. The structural and microstructural properties were determined by x-ray diffractometry (XRD), Fourier transform infrared spectroscopy (FTIR) and transmission electron microscopy (TEM). X-ray photoelectron spectroscopic (XPS) studies were done for determining the chemical states of silver in the silica matrix. For the lowest $AgNO_3$ concentration, monodispersed and spherical Ag crystallites, with an average diameter of 5 nm, were obtained. Grain growth and an increase in size distribution was observed for higher concentrations. The occurrence of surface plasmon resonance (SPR) bands and their evolution in the size range 5–10 nm is studied. For decreasing nanoparticle size, a redshift and broadening of the plasmon-related absorption peak was observed. The observed redshift and broadening of the SPR band was explained using modified Mie scattering theory.

(Some figures in this article are in colour only in the electronic version)

## 1. Introduction

Optical properties of composites consisting of nanometric-sized metal particles dispersed in solid dielectric materials such as glass have been receiving increasing attention because of their important applications in areas such as optical energy transport, polarizers and as color filters in liquid crystal displays and as photonic crystals [1]. Noble metal nanoparticles can be introduced into a glass matrix through different methods of preparation such as melt quenching, ion implantation, ion exchange and sol–gel techniques. These metal clusters are known to exhibit a very intense color, which is absent in the bulk material as well as in individual atoms. Their origin is attributed to the collective oscillation of the free conduction electrons induced by an interacting electromagnetic field. These resonances are also denoted as surface plasmons. The plasmonic coupling of metal nanoparticles with light enhances a broad range of useful optical phenomena, such as resonant light scattering (RLS), surface plasmon resonance (SPR) and surface-enhanced Raman scattering (SERS), all of which have tremendous application potential in areas such as in ultra-sensitive chemical and biomolecular detection and analysis [2, 3].

Among various methods for the synthesis of silver–silica nanocomposites, the sol–gel process needs special mention because of the low processing temperature, high purity and homogeneity of the resultant products. Moreover, the initial sol can be converted into fiber, thin films or a dense ceramic depending on the nature of the applications. The most common method for the preparation of $Ag–SiO_2$ nanocomposites is the post-synthesis impregnation of pure or organic functionalized mesoporous host silica with $AgNO_3$ solutions. Subsequent thermal reduction is performed to produce metallic silver nanoparticles. Several reports exist in the literature pertaining to this method of preparation [4, 6, 7]. Cai *et al* [4] reported the preparation of nanosized silver particles within the pores of mesoporous silica. The mean particle size was about 3 nm. Exposure of the composites to the ambient air resulted in the

[4] Author to whom any correspondence should be addressed.

 

formation of a thin layer of silver oxide on the surface of the silver nanoparticles and this resulted in the damping of surface plasmon resonance. Chen *et al* [7] obtained Ag nanoparticles by the decomposition of silver nitrate within the pores of mesoporous silica. The average particle size varied from 5 to 10 nm. Plasmon resonance was not observed in this case but a large redshift of the absorption edge was noticed with the loading of Ag particles. The non-observance of SPR bands in these investigations is probably due to the interactions of the nanoparticles with the pore walls and also due to adsorbed silver oxides on the nanoparticles. However, the addition of silver salts to a precursor of silica at the very initiation of the sol–gel process can result in Ag–$SiO_2$ nanocomposites free from silver oxides. Garcia *et al* [8] obtained oxide-free thin films of silver silica composites by this method. But their main focus was on the photoluminescence properties of such films. The Ag clusters formed in the silica matrix may be stable only for a few days. The instability can be attributed to the diffusion of atmospheric oxygen into the silica network. Hence, the degradation of the SPR band with time is unavoidable in these types of composites. Recent studies by Hu *et al* indicate that the SPR band vanishes completely after heat treatment in ambient air for half a second [9]. However, better stability can be attainable for bigger particles [6].

What is evident from these studies is that, while some researchers have prepared Ag–$SiO_2$ nanocomposites for observing SPR bands, they were only partially successful in their attempts because either silver is converted to silver oxide or the metallic silver present is short lived, which leads to transient bands. At the same time, though others like Garcia *et al* were successful in synthesizing a pure Ag–$SiO_2$ nanocomposite, the focal theme of their investigation was on the photoluminescence properties of these composites.

Mie was the first to describe the plasmon resonance quantitatively by solving Maxwell's equations with the appropriate boundary conditions for spherical particles. Mie scattering theory has remained important for so long that it is the only simple and exact solution to Maxwell's equations that is relevant to spherical and well-separated particles. Moreover, most of the preparation techniques yield particles that are approximately spherical in shape. This leads to results that can be modeled reasonably well using this theory. For nanoparticles whose size regime is very much smaller than the wavelength of the exciting source of light, it is assumed that only the dipole absorption of the Mie equation contributes to the extinction cross section of the nanoparticles. The extinction cross section represents loss of energy from the incident electromagnetic wave due to both scattering and absorption. The Mie scattering theory then reduces to the following form [2]:

$$C_{\text{ext}} = \frac{24\pi^2 R^3}{\lambda} \varepsilon_m^{\frac{3}{2}} \frac{\varepsilon''}{(\varepsilon' + 2\varepsilon_m)^2 + \varepsilon''^2}. \quad (1)$$

Here $C_{\text{ext}}$ is the extinction cross section for the nanoparticles dispersed in a medium, $R$ is the radius of the particle, $\lambda$ is the wavelength of the electromagnetic wave and $\varepsilon = \varepsilon' + i\varepsilon''$ is the complex dielectric function of the metal particle embedded in the surrounding matrix with a dielectric constant $\varepsilon_m$. Within the dipole approximation there is no size dependence except for varying intensity. Experimentally, however, one observes a strong size dependence on the plasmon bandwidth and peak position. Researchers have observed the SPR band shifts to both higher and lower energies for decreasing particle dimensions. For silver nanoparticles classical conductivity models predict redshifts due to the increased damping of the electron motion with decreasing size [10, 11]. However, blueshifts because of quantum size effects have also been observed [12].

It is thus evident from these literature reports that the findings of researchers are at variance and inconsistent. Such a scenario has motivated these authors to initiate a systematic study on Ag–$SiO_2$ nanocomposites looking at the size-dependent variation of SPR bands afresh, with particular emphasis on synthesizing Ag–$SiO_2$ nanocomposites free from silver oxides. Any thorough investigation on such a system needs confirmatory evidence for the existence of Ag as pure elemental silver. In addition to relying on conventional techniques like XRD, emphasis was laid in probing the presence of Ag using x-ray photoelectron spectroscopy (XPS). It is also known that increasing the concentration of Ag in the $SiO_2$ matrix enhances the particle size and so also the particle agglomeration. Hence, evaluation of particle size using a technique like transmission electron microscopy (TEM) is a prerequisite for correlating the results. Moreover, modeling the experimental results in Ag–$SiO_2$ nanocomposites will give credence to the evolution of SPR bands with size in these nanocomposites.

In this investigation the Ag–$SiO_2$ nanocomposite is synthesized by the sol–gel technique using tetraethyl orthosilicate (TEOS) and silver nitrate ($AgNO_3$) as precursors. The silver nitrate concentration was varied to obtain composites with different nanoparticle sizes. The occurrence of SPR bands and their evolution with size is also studied. The experimental data will be model fitted by the modified Mie scattering theory that ensures size-dependent variation in dielectric function of the metal nanoparticles.

## 2. Experiment

### 2.1. Preparation

Ag–$SiO_2$ nanocomposites were prepared using an Ag–$SiO_2$ sol and employing tetraethyl orthosilicate (TEOS), ethanol ($C_2H_5OH$), distilled water and silver nitrate as precursors. Here ethanol was used as a solvent. A few drops of dilute nitric acid ($HNO_3$) were added as a catalyst for promoting hydrolysis. The pH of the mixture was maintained at 2. The assumed molar ratios of TEOS/ethanol/$H_2O$/$AgNO_3$ were $1/2/5/n$, respectively. $n$ is the nominal molar ratio of Ag/Si, which was chosen to be 0.02, 0.04 and 0.06, respectively. The mixture was continuously stirred using a magnetic stirrer until a completely miscible solution was obtained. The resulting viscous sol was poured into a Petri dish and was tightly covered. Holes were pierced in the cover of the dishes. The dishes were then kept in an hot air oven at 45 °C. The aging period was 15 d. The monoliths thus obtained were heat treated

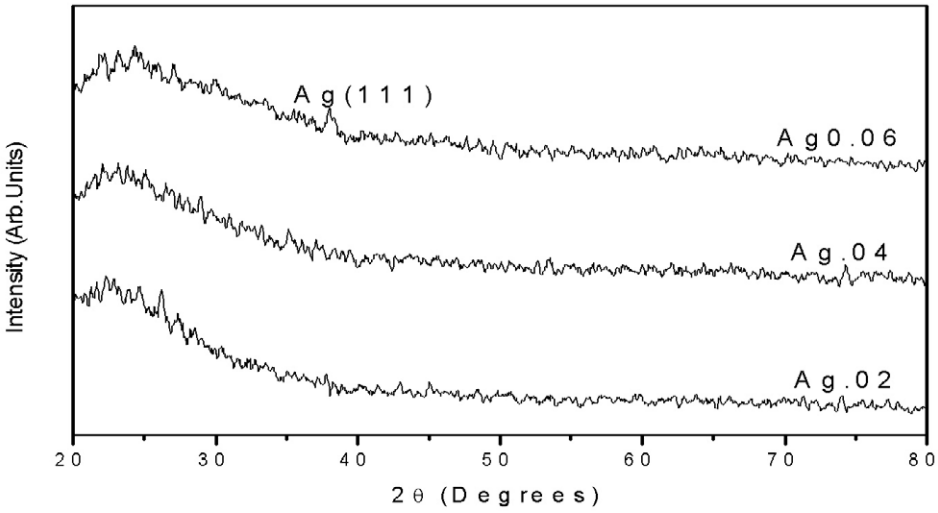


**Figure 1.** XRD pattern for Ag–$SiO_2$ composites.

at 500 °C in air for 4 h to obtain Ag–$SiO_2$ nanocomposite powders. The samples obtained are coded as Ag 0.02, Ag 0.04 and Ag 0.06 for Ag concentrations corresponding to 0.02, 0.04 and 0.06, respectively.

### *2.2. Characterization*

The structural parameters of the Ag–$SiO_2$ composites were evaluated using an x-ray powder diffractometer technique employing a copper target (Cu K$\alpha$ = 1.5418 Å, Rigaku $D_{max}$ C). The scanning speed was adjusted to 2° $min^{-1}$ with a sampling interval of 0.05. Transmission electron microscopy observations were carried out in a FEI Tecnai $G^2$ 30 S-TWIN electron microscope operated at 300 kV. The microscope had a point resolution of 2 Å. A Thermo Nicolete Avatar 370 DTGS model spectrophotometer was used in recording the FTIR spectra of the samples in the range 400–4000 $cm^{-1}$. The spectrum was collected after 32 scan repetitions with a resolution of 4 $cm^{-1}$. X-ray photoelectron spectroscopy (XPS) measurements were carried out using an Omicron Nanotechnology Multiprobe Instrument. XPS spectra were obtained using a high resolution hemisphere analyzer EA 125 HR equipped with a detection system consisting of seven channeltrons. A monochromated Al K$\alpha$ source of $h\nu$ = 1486.6 eV was used to probe an Ag–$SiO_2$ attached by double-sided tape to the molybdenum sample holder. Pressure in the XPS chamber during the measurements was $5 \times 10^{-10}$ mbar and the instrumental total resolution was 0.6 eV. Charge compensation was provided by electron gun flooding with a bias voltage of 8.4 V and a filament current of 1.1 A. The emission current was 10 $\mu$A. The binding energies were corrected by C 1s as reference energy (C 1s = 284.8 eV) [13]. C 1s had an FWHM of 2 eV. A wide scan was collected to ensure that no foreign materials were present on the sample surface. Narrow scans of the Ag 3d and O 1s regions were collected at an analyzer pass energy of 20 eV after 20 scan repetitions with a measuring step of 0.01 eV. The quality of the charge-compensated wide scan and narrow scan XPS spectra was checked several times by observing the position, intensity and FWHM of the well-known XPS peaks. Curve fitting to the XPS spectrum was done using CasaXPS software. Background subtraction was done using the Shirley method. The diffuse reflectance spectra of the samples were recorded in a Jasco V 570 UV–vis spectrophotometer in the wavelength range 325–800 nm with 1 nm resolution. The absorption spectrum was obtained from the measured reflectance using the Kubelka–Monk relation [5].

## 3. Results and discussion

Figure 1 shows the XRD pattern for the Ag–$SiO_2$ composites for different loadings of Ag. The diffraction patterns for all the composites are characterized by a broad peak centered at around $2\theta$ = 23° which is characteristic of amorphous $SiO_2$. Even though silica is non-crystalline the broad peak is due to the short-range order present. Characteristic peaks representing pure Ag were not very prominent in the samples with low concentrations of Ag. However, as the concentration of Ag increased a peak corresponding to the diffraction from the Ag (111) plane is observed at $2\theta = 38°$.

Figure 2(a) shows the TEM image of Ag 0.02. It can be seen that the nanoparticles are spherical in shape and are well separated. In figure 3(a), the histogram of the particle sizes obtained from figure 2(a) is shown. The solid line corresponds to a Gaussian function fitted to the experimental data. The mean particle size and standard deviation obtained from the fit was 5.5 and 1.3 nm, respectively. The electron microscopy image of Ag 0.06 is shown in figure 2(b). From the histogram of the particle size in figure 3(b) it is clear that an increase in the concentration of silver nitrate has resulted in the grain growth and agglomeration as well as in a wide size distribution of the nanoparticles. Detailed HRTEM was conducted to determine the nature of the nanocrystallites (figure 4). Lattice planes of the nanocrystallites are clearly visible in the high resolution image. This corresponds to Ag(111) which was also seen in the XRD.

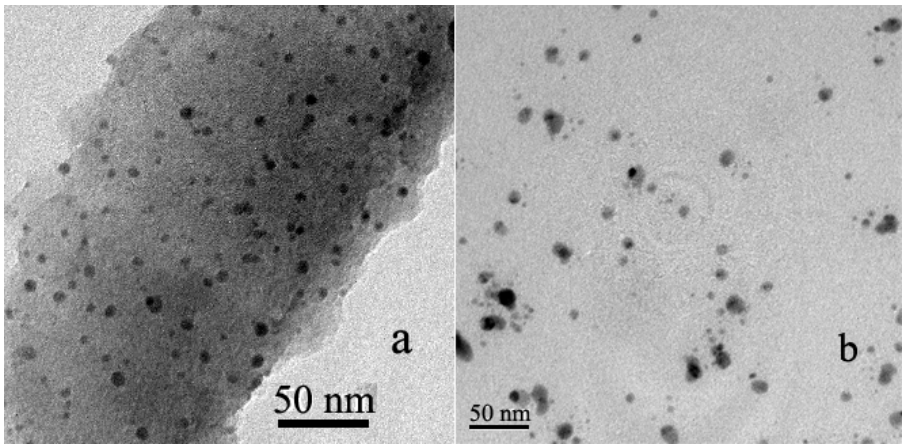


**Figure 2.** TEM image of (a) Ag 0.02 and (b) Ag 0.06.

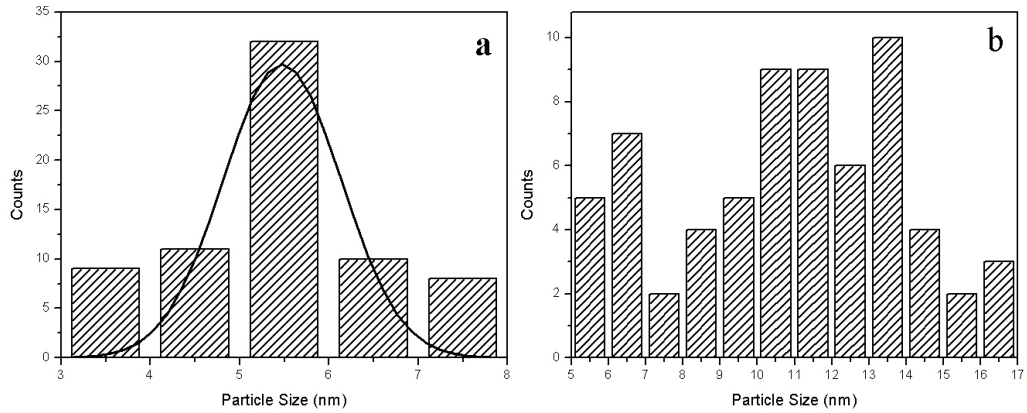


**Figure 3.** Histogram of the particle sizes obtained from the transmission electron micrograph of (a) Ag 0.02 and (b) Ag 0.06.

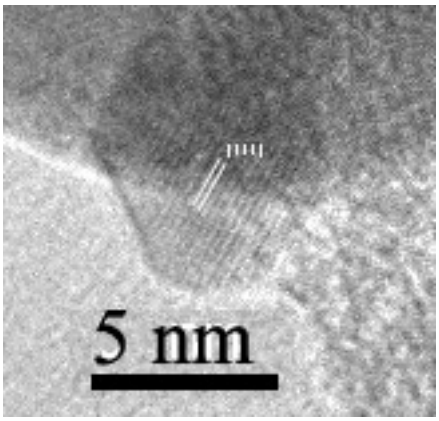


**Figure 4.** HRTEM image of Ag 0.02.

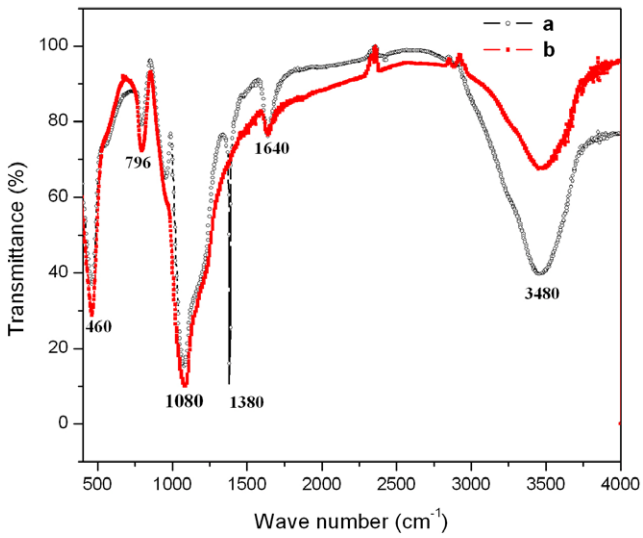


**Figure 5.** FTIR spectrum of Ag 0.02 (a) before and (b) after heat treatment at 500 °C.

The IR spectrum for Ag 0.02 obtained before and after heat treatment at 500 °C was plotted and is shown in figure 5. The spectrum is characterized by three main absorption bands assigned to three different vibrational modes of the Si–O–Si bonds. The lowest frequency mode (∼460 $cm^{-1}$) is assigned to the transverse-optical (TO) rocking motions perpendicular to the Si–O–Si plane, of the oxygen bridging two adjacent Si atoms. At around 800 $cm^{-1}$ a weak band due to symmetric stretching of the O atom along a line bisecting the Si–O–Si angle is observed. The highest frequency mode, which

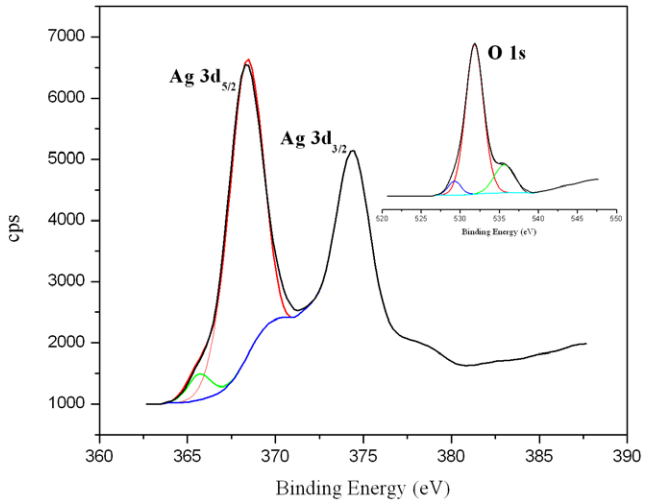


**Figure 6.** Ag 3d XPS spectra for the Ag 0.02 composite. The inset shows the corresponding O 1s XPS spectra.

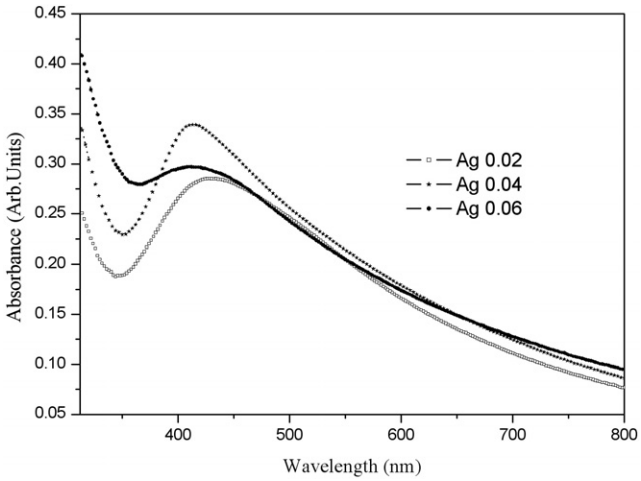


**Figure 7.** Absorption spectrum for the composites.

is at 1080 $cm^{-1}$, is associated with the back and forth motion of the oxygen atom along a line parallel to the Si–Si axis. This motion results in the opposite distortion of two neighboring Si–O bonds [14]. The characteristic $\nu_s$(Si–(OH)) vibration at 955 $cm^{-1}$ was also found in the IR spectra of uncalcined samples. This band disappears after calcination. This disappearance of the characteristic peak corresponding to Si–OH is accompanied by an increase in intensity of the peak corresponding to $SiO_2$. This provides evidence to the fact that the silica matrix gets structurally ordered as the temperature of firing increases. The band at 1640 $cm^{-1}$ corresponds to the bending of the absorbed $H_2O$ molecules, which can interact through hydrogen bonds with silanol groups. The characteristic band for stretching (OH) groups was found to be at around 3480 $cm^{-1}$ [15]. The intensity of this band decreased with heat treatment. It may be noted that a strong band at around 1380 $cm^{-1}$ was observed in the IR spectra of the fresh sample. This is due to nitrate ions and this band disappears at 500 °C, indicating the decomposition of $AgNO_3$ [16].

It has been reported that silver in mesoporous silica when exposed to ambient air gets oxidized. Geoffry *et al* [17] reported that $Ag_2O$ is characterized by the infrared bands at 540 and 645 $cm^{-1}$, while AgO is characterized by bands at 951 and 986 $cm^{-1}$. Cai *et al* [4] observed a band at 1450 $cm^{-1}$ due to $Ag_2O$ in silver–silica nanocomposites. However, in our case, no characteristic IR bands corresponding to $Ag_2O$ or AgO were noticeable in the spectrum. These observations point to the fact that Ag is present in the pure elemental form and also any oxides present may be in minute concentrations to be detected by the spectrometer.

Further XPS analysis confirms the presence of Si, O and Ag in the composites. Figure 6 shows the Ag 3d core-level emission from the Ag 0.02 composite. The spectrum exhibits a typical Ag 3d doublet at a binding energy of 368.4 eV with a doublet splitting of 6 eV. The position of these peaks indicates that silver is present as $Ag^0$. The minor peak located at around 377 eV corresponds to the surface plasmon loss peak of silver [22]. Curve fitting to the peaks was done to trace out the presence of silver oxides, if any. From the Ag 3d spectrum it is seen that a hump is located at the tail of the metallic peak. This minor peak is centered on 366 eV and its percentage contribution is 4.2. It should be noted that the reported binding energies of $Ag_2O$ and AgO are at 367.8 and 367.4 eV, respectively [8, 18]. In order to clarify the origin of this minor peak the O 1s spectrum from the same sample was collected. The inset of figure 6 shows the O 1s spectrum. The peak fitting indicates that the spectrum can be resolved into three components, of which the main one located at 532 eV is from $SiO_2$. The minor peak at 535 eV is from bounded water which has further confirmations from the FTIR spectrum. The other peak, which is situated at around 529.2 eV, is due to $Ag_2O$. The percentage concentration of this component is 5. Bearing this in mind one can infer that the minor peak in the Ag 3d located at 366 eV comes from $Ag_2O$ and its origin can be from the exposure of the composites to the ambient air.

Figure 7 depicts the absorption spectrum for the composites. It can be seen that the absorption of the composite has a strong dependence on the Ag loading amount. The sample Ag 0.04 exhibits a strong absorption peak at around 410 nm which is a well-known SPR absorption of Ag nanoparticles in silica [9]. Broadening of the plasmon band along with a redshift in peak position was observed for Ag 0.02. When the Ag/Si molar ratio was increased to 0.06, the plasmon band was suppressed. The electron micrograph corresponding to Ag 0.06 clearly shows the agglomeration of the nanoparticles. Therefore, the interaction between the nanoparticle cannot be disregarded and this interaction suppresses the surface plasmon absorption.

The intense absorption band at around 410 nm is due to the collective oscillation of all free electrons in the silver particles resulting from the interaction with electromagnetic radiation. The electric field of the incoming radiation induces the formation of a dipole in the nanoparticle. A restoring force in the nanoparticle tries to compensate for this, resulting in a unique resonance wavelength. The oscillation wavelength depends on a number of factors among which particle size and shape as well as the nature of the surrounding medium are the most prominent among them.

In the simplified case of a metal nanosphere with radius $R$ much smaller than the incident wavelength (a condition commonly referred to as the quasi-static approximation), the plasmon response is essentially dipolar in nature. The strength and frequency of this resonance is related to the total number of electrons in the oscillating dipole (defined essentially by the particle volume or $R^3$), the complex dielectric function $\varepsilon$ ($\omega$) and the dielectric constant of the local medium $\varepsilon_m$.

The dipolar plasmon response of the nanoparticles is often defined by its polarizability, which can be expressed in terms of the above-mentioned parameters by the electrostatic Clausis–Mossotti equation (also known as the Lorentz–Lorenz equation)

$$\alpha = 4\pi\varepsilon_0 R^3 \frac{(\varepsilon - \varepsilon_m)}{(\varepsilon + 2\varepsilon_m)}. \tag{2}$$

Here $\varepsilon$ and $\varepsilon_m$ are, respectively, the wavelength-dependent dielectric functions of the material comprising the particle and its ambient.

The resonance condition leading to maximum polarization is $\varepsilon + 2\varepsilon_m = 0$, requiring $\varepsilon(\omega)$ to be negative. However, the complex dielectric function may be divided into real and imaginary components $\varepsilon'(\omega)$ and $\varepsilon''(\omega)$ in order to remove the phase-dependent term from the equation; resonance is thus achieved when $\varepsilon'(\omega) = -2\varepsilon_m$ and $\varepsilon''(\omega) \ll 1$. The dielectric function is negative when $\omega$ is below some threshold frequency $\omega_p$, known also as the plasma frequency. The relationship between $\varepsilon(\omega)$ and $\omega_p$ can be illustrated by the Drude model, a conceptually useful description of free-electron behavior in metals. Here $\varepsilon'(\omega)$ and $\varepsilon''(\omega)$ can be approximated in terms of $\omega_p$ and $\gamma$, the plasma relaxation frequency:

$$\varepsilon = \varepsilon' + i\varepsilon'' = 1 - \frac{\omega_p^2}{\omega^2 + \gamma^2} + i\frac{\omega^2\gamma}{\omega(\omega^2 + \gamma^2)}. \tag{3}$$

Exact solutions for the optical properties of metal nanostructures can be obtained from Mie solutions to Maxwell's equations (equation (1)). Application of Mie scattering theory requires the input of $\varepsilon_m$ and $\varepsilon$ ($\omega$). $\varepsilon$ ($\omega$) is given by equation (3) with

$$\omega = 2\pi\frac{c}{\lambda} \qquad \text{and} \qquad \gamma = \frac{V_f}{L}.$$

Here $V_f$ is the Fermi velocity of the electrons, $L$ is the mean free path length in the bulk material and $c$ is the velocity of light.

For metal particles with radius $R$ smaller than the mean free path $L$ of conduction electrons in the bulk metal, the mean free path can be dominated by collisions with the particle boundary. Thus the damping constant ($\gamma$) in Drude theory, which is the inverse of the collision time for conduction electrons, is increased because of additional collisions with the boundary of the particle [20]. Under the assumption electrons are diffusely reflected at the boundary, $\gamma$ can be written as

$$\gamma = \frac{V_f}{L} + \frac{V_f}{R}. \tag{4}$$

The experimental extinction spectra corresponding to Ag 0.04 and Ag 0.02 was simulated using Mie scattering theory (combining equations (1), (3) and (4)). For silver nanoparticles we have used the values of $V_f = 1.38 \times 10^6$ m s$^{-1}$, $L = 57$ nm and $\omega_p = 1.39 \times 10^{16}$ s$^{-1}$ [12, 19]. $R$ is taken as a fitting parameter. Figure 8 shows the experimental and simulated absorption spectra.

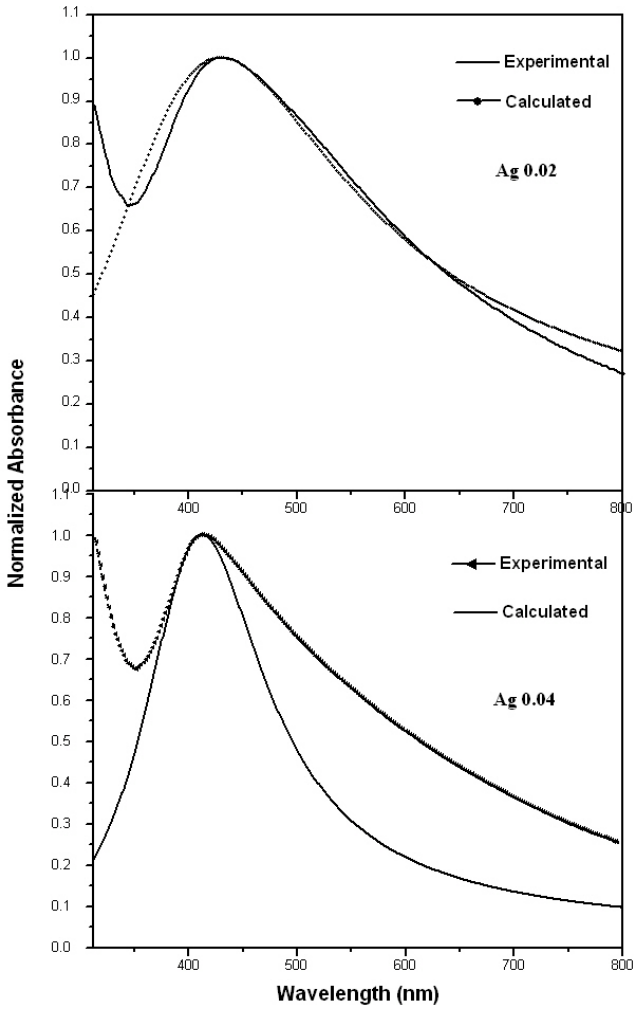


**Figure 8.** Mie simulation for the composite Ag 0.02 and Ag 0.04.

The nanoparticles size obtained from the curve fitting was 6 and 10 nm for Ag 0.02 and Ag 0.04, respectively. The obtained particle size was in agreement with the electron microscopy observations. The observed changes in the SPR curve can be related to the size effects. Strong absorption centered at around 410 nm is found to be redshifted and broadened when the size of the particle is reduced from 10 to 5 nm. For silver nanoparticles, redshifts due to damping of electron motion with decreasing size are predicted with classical models and have been observed. Ag clusters in stained glass show a redshift amounting to 10 nm upon decreasing the size from 20 to 2 nm [11]. Taleb and coworkers using thiol-passivated Ag clusters observed a redshift and broadening with decreasing size [21]. They found that the plasmon band shifts from 425 to 450 nm as the size is reduced from 3.8 to 2.3 nm. Wilcoxan and coworkers also observed a redshift and broadening of the SPR band with decreasing particle size [10]. The redshift from 410

to 430 nm in the present case is comparable with that of earlier observations. It should be noted that the contributions of interband transitions to the absorption spectra were not considered while simulating the experimental data. Moreover the effect of particle size distribution was also neglected while modeling the experimental absorption spectra. Thus, one can observe that a combination of Mie scattering theory and free electron contribution to the dielectric function, suitably modified to include the mean free path limitation, describes the experimental observation more or less faithfully with a slight departure on the higher-wavelength regime.

## 4. Conclusion

Ag–$SiO_2$ nanocomposites were obtained by the sol–gel method. X-ray photoelectron spectroscopy studies showed that the silver nanoparticles in the silica matrix were in the pure elemental form along with traces of $Ag_2O$. The size evolution of their optical properties was evaluated in the range 5–10 nm. The redshift and broadening of the surface plasmon band with a decrease in size is in agreement with the classical models. An increase in the Ag quantity can result in the damping of the surface plasmon band due to the dipolar interaction between the silver nanoparticles. This method of synthesis of Ag–$SiO_2$ nanocomposites can be adapted for the preparation of other noble metal–$SiO_2$ nanocomposites. Further it would be worthwhile to apply these models to such systems to gage the particle size range under which these composites exhibit SPR resonance bands.

## Acknowledgments

ST and MRA acknowledge the Inter University Accelerator Centre, New Delhi for financial assistance in the form of a project UFUP no. 35306. MRV acknowledges the Department of Science and Technology, New Delhi for providing the HRTEM facility at NIIST, Thiruvananthapuram.

## References

[1] Baker C C, Pradhan A and Ismat Shah S 2004 *Encyclopedia of Nanoscience and Nanotechnology* vol 5, ed H S Nalwa (California: American Scientific Publishers) p 463
[2] Wei A 2004 *Nanoparticles—Building Blocks for Nanotechnology* ed V Rotello (New York: Kluwer–Academic/Plenum) p 174
[3] Moores A and Geottmann F 2006 *New J. Chem.* **30** 1121
[4] Cai W, Tan M, Wang G and Zhang L 1996 *Appl. Phys. Lett.* **69** 2980
[5] Sirita J, Phanichphant S and Meunier F C 2007 *Anal. Chem.* **79** 3912
[6] Cai W, Zhang Y, Jia J and Zhang L 1996 *Appl. Phys. Lett.* **73** 2709
[7] Chen W and Zhang J 2003 *Scr. Mater.* **49** 321
[8] Garcia M A *et al* 2004 *J. Appl. Phys.* **96** 3737
[9] Hu J, Lee W, Cai W, Tong L and Zeng H 2007 *Nanotechnology* **18** 185710
[10] Wilcoxon J P, Martin J E and Porencio P 2001 *J. Chem. Phys.* **115** 998
[11] Smithard M A and Dupree R 1972 *Phys. Status Solidi* a **11** 695
[12] Mandal S K, Roy R K and Pal A K 2002 *J. Phys. D: Appl. Phys.* **35** 2198
[13] Moulder J F, Stickle W F, Sobol P E and Bomben K D 1992 *Handbook of X-ray Photoelectron Spectroscopy* ed J Chastain (Minnesota: Perkin-Elmer) p 14
[14] Thomas S, Sakthikumar D, Joy P A, Yoshida Y and Anantharaman M R 2006 *Nanotechnology* **17** 5565
[15] Bruni S, Caraiti F, Casu M, Lai A, Musinu A, Piccaluga G and Solinas S 1999 *Nanostruct. Mater.* **11** 573
[16] Moreno E M, Zayat M, Morales M P, Serna C J, Roig A and Levy D 2002 *Langmuir* **18** 4972
[17] Water House G I N, Bowmaker G A and Metson J B 2001 *Phys. Chem. Chem. Phys.* **3** 3838
[18] www.srdata.nist.gov/xps
[19] Chatterjee A and Chakravorty D 1989 *J. Phys. D: Appl. Phys.* **22** 1386
[20] Bohren C F and Huffman R R 1998 *Absorption and Scattering of Light by Small Particles* (New York: Wiley–Interscience) p 337
[21] Taleb A, Petit C and Pileni M P 1997 *Chem. Mater.* **9** 950
[22] Tachibana Y, Kusunoki K, Watanabe T, Hashimoto K and Ohsaki H 2003 *Thin Solid Films* **442** 212